Journal of Zhejiang University SCIENCE
ISSN 1009-3095
http://www.zju.edu.cn/jzus
E-mail: jzus@zju.edu.cn

JZUS

Strengthening reinforced concrete beams using prestressed glass fiber-reinforced polymer–Part II: Analytical study

HUANG Yue-lin†, HUNG Chien-hsing, YEN Tsong, WU Jong-hwei, LIN Yiching

(*Department of Civil Engineering, National Chung-Hsing University, 40227, Taiwan, China*)

†E-mail: ylhuang@dragon.nchu.edu.tw

Received Aug. 12, 2004; revision accepted Nov. 16, 2004

Abstract: Strengthening reinforced concrete (R. C.) beams using prestressed glass fiber-reinforced polymer (PGFRP) was studied experimentally as described in Part I of this paper (Huang *et al*., 2005). In that paper, R. C. beams, R. C. beams with GFRP (glass fiber-reinforced polymer) sheets, and R. C. beams with PGFRP sheets were tested in both under-strengthened and over-strengthened cases. The test results showed that the load-carrying capacities (ultimate loads) of the beams with GFRP sheets were greater than those of the beams without polymer sheets. The load-carrying capacities of beams with PGFRP sheets were greater than those of beams with GFRP sheets. The objective of this work is to develop an analytical method to compute all of these load-carrying capacities. This analytical method is independent of the experiments and based only on the traditional R. C. and P. C. (prestressed concrete) theory. The analytical results accorded with the test results. It is suggested that this analytical method be used for analyzing and designing R. C. beams strengthened using GFRP or PGFRP sheets.

Key words: Analytical analysis, Glass fiber-reinforced polymer, Prestressed glass fiber-reinforced polymer, R. C. beams
doi:10.1631/jzus.2005.A0844 **Document code:** A **CLC number:** TU411

INTRODUCTION

When the flexural load-carrying capacities of existing R. C. or P. C. structures are not sufficient for the service loads, structural strengthening becomes necessary. Using steel plates to strengthen concrete members is a traditional method (Raithby, 1980) and is still an important and popular way at the present time. Fiber-reinforced polymer (FRP) sheets and plates have been used recently as an alternative to steel plates for strengthening concrete structures because their noncorrosive characteristics offer a promising solution to durability problems caused by steel corrosion (ACI 440, 1996). Saadatmanesh and Ehsani (1991) were the first to use prestressed GFRP sheets. They prestressed the beams by cambering them upward using an upside down load and then bonding the plates to the beam's tension faces. Triantafillou *et al*.(1992) first used independent equipment to prestress CFRP sheets to strengthen concrete members. Part I of this paper (Huang *et al*., 2005) focused on prestressed GFRP (glass fiber-reinforced polymer) sheets using independent equipment in an experimental study. Part II of this paper focuses on the analytical study.

Very few analytical studies on strengthening of R. C. beams with epoxy-bonded fiber composite plates are reported in the literature. An *et al*.(1991) first proposed an analytical and parametric study on R. C. beams strengthened with FRP plates. However, they did not perform tests to verify the exactness of their analytical method. All of the experimental results in Part I of this paper (Huang *et al*., 2005) were checked and compared with the suggested analytical method herein. Garden *et al*.(1996) performed a parameter study on strengthening of reinforced concrete beams with bonded composites but they did not address prestressed FRP plates. Wong and Vecchio (2003) presented a finite element analysis method for modeling externally reinforced structural members

with polymer strips but their analysis was not a theoretical analysis. This paper suggests a theoretical analysis method for the evaluation of R. C. beams strengthened with normal GFRP plates and prestressed GFRP plates. Grace and Singh (2003) offered a similar theoretical approach for carbon fiber-reinforced polymer prestressed (CFRP) beams. In that paper, the CFRP's were used as prestressed tendons. In this work, the GFRP plates were used as an externally bonded enhancement material. Several advanced countries have developed specifications (ACI 318, 1999; CHBDC, 2000; JSCE, 1997) for guidelines on using composite polymers. To carry out this type of work, a theoretical and more reliable approach for the analysis and design of beams strengthened with polymer plates is needed. In 1999, a Richter scale magnitude 7.3 earthquake occurred at Chi-Chi, Taiwan. This earthquake caused nearly 3000 deaths and severely damaged or collapsed more than 100 high rise buildings. Afterwards, most of the damaged buildings were repaired using FRP sheets. But so far, there are few references on an analytical approach for the engineering purposes. A theoretical analysis method is needed for the design or analysis for R. C. structural rehabilitation. The analytical study described in this article may offer some help on this subject.

ANALYTICAL METHODS

Basic assumptions

The following assumptions were made in developing the proposed analytical method: (1) The concrete tensile strength is neglected; (2) The stress-strain relationship of the steel is considered elastically perfect; (3) The steel and contact concrete have the same strain; (4) Plane sections remain plane after bending; (5) Complete composite action between the GFRP and PGFRP sheets and concrete exists.

Two types of beams, T-shaped and ⊥-shaped were experimented with in our work described in Part I of this paper (Huang *et al*., 2005). The T-shaped beams shown in Fig.1 in (Huang *et al*., 2005) were considered under-strengthened beams, meaning that all of the beams, reference beams or beams strengthened using GFRP or PGFRP sheets, would fail on the tension faces (bottom faces). The ⊥-shaped beams shown in Fig.3 in (Huang *et al*., 2005) were considered over-strengthened beams, meaning that the reference beams would fail on the tension faces while the strengthened beams would all fail on the compression faces (top faces). The test specimens for each type of beam in Part I included reference beams, beams strengthened with GFRP sheets and beams strengthened with PGFRP sheets. The specimen details were described in Part I (Huang *et al*., 2005). The main purpose of the work described in Part II here is to develop an analytical method to compute and check the Part I test results.

Analytical method for T-shaped beams without GFRP sheets

For T-shaped beams without GFRP sheets, the compression distribution on the concrete is assumed to be a rectangular shape (Wang and Salmon, 1998). The following cases are considered.

1. If the neutral axis is above h_f/β_1

Referring to Fig.1, if the neutral axis (N. A.) is above h_f/β_1 (h_f is the thickness of the flange), the compression zone is entirely in the flange area, and if the strain of the compression steel is $\varepsilon_s' = \dfrac{\varepsilon_c^u (x-d')}{x} < \varepsilon_y$, the stress of the compression steel will be $f_s'=E_s\varepsilon_s'$. According to the equilibrium equation $C_c+C_s=T$,

$$0.85 f_c' b \beta_1 x + A_s' E_s \frac{\varepsilon_c^u (x-d)}{x} = A_s f_y \tag{1}$$

the neutral axis value of x can then be determined and the nominal moment M_n is

$$M_n = 0.85 f_c' b \beta_1 x (d - \beta_1 x/2) + A_s' f_s' (d - d') \tag{2}$$

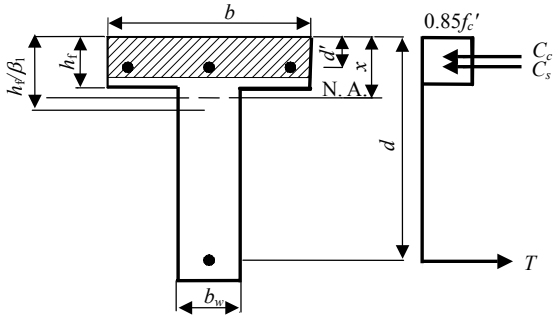

Fig.1 Stress distribution of T-shaped beams without GFRP sheets but with N. A. above h_f/β_1

where $\beta_1 = 0.85 - 0.05\left(\frac{f_c' - 28}{7}\right)$; f_c', compression strength of concrete (MPa); ε_c^u, concrete ultimate strain, 0.003; d', location of compression steel; d=effective beam depth; ε_y, yield strain of steel, $\varepsilon_y = f_y/E_s$; f_y, yield strength of steel; E_s, steel Young's modulus; C_c, compression force resultant of concrete; C_s, compression force resultant of steel; T, total tension force; b, beam's flange width; b_w, beam web width; A_s', area of compression steel; A_s, area of tension steel.

If the strain of the compression steel is $\varepsilon_s > \varepsilon_y$, the steel stress is f_y. According to the equilibrium equation $C_c + C_s = T$,

$$0.85 f_c' b \beta_1 x + A_s' f_y = A_s f_y \tag{3}$$

the value of x can then be determined and the nominal moment is

$$M_n = 0.85 f_c' b \beta_1 x (d - \beta_1 x/2) + A_s' f_y (d - d') \tag{4}$$

2. If N. A. is below h_f/β_1

If N. A. is below h_f/β_1, as shown in Fig.2, the compression zone includes the entire flange area and part of the web area. If the strain of the compression steel is $\varepsilon_s' = \frac{\varepsilon_c^u (x - d')}{x} < \varepsilon_y$, the steel stress will be $f_s' = E_s \varepsilon_s'$. According to the equilibrium equation $C_c + C_s = T$,

$$0.85 f_c'(b - b_w) h_f + 0.85 f_c' b_w \beta_1 x + A_s' E_s \frac{\varepsilon_c^u (x - d')}{x} = A_s f_y \tag{5}$$

the value of x can then be determined and the nominal moment is

$$M_n = A_s' f_s'(d - d') + 0.85 f_c' b_w \beta_1 x (d - \beta_1 x/2) + 0.85 f_c'(b - b_w) h_f (d - h_f/2) \tag{6}$$

If the strain of the compression steel is $\varepsilon_s > \varepsilon_y$, the steel stress will be $f_s = f_y$. According to the equilibrium equation $C_c + C_s = T$,

$$0.85 f_c'(b - b_w) h_f + 0.85 f_c' b_w \beta_1 x + A_s' f_y = A_s f_y \tag{7}$$

the value of x can then be determined and the nominal moment capacity is

$$M_n = A_s' f_y (d - d') + 0.85 f_c' b_w \beta_1 x (d_c' - \beta_1 x/2) + 0.85 f_c'(b - b_w) h_f (d - h_f/2) \tag{8}$$

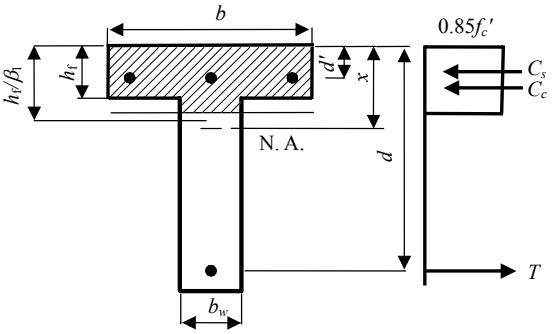

Fig.2 Stress distribution of T-shaped beams without GFRP sheets but with N. A. below h_f/β_1

Analytical method for T-shaped beams with GFRP sheets

According to the failure behavior in the tests in the work described in Part I of this paper (Huang *et al*., 2005), the following assumptions are made for the analysis of T-shaped beams with GFRP sheets: (1) Complete composite action take places between GFRP sheet and concrete; (2) T-shaped beams always fail on the tension faces; (3) The GFRP sheets fail first; (4) The compressive concrete on the top never reaches its ultimate strain.

According to Assumptions (3) and (4), because the T-shaped beams with GFRP sheets always fail on the GFRP sheets, the strain on the concrete top never reaches the value 0.003. The concrete compression stress distribution is not assumed as a rectangular shape and the compression resultant force of the concrete should be obtained by integrating the stress distribution rather than using the $0.85 f_c' ba$ value. In this case, N. A. location can also be determined based on the static equilibrium relation, and then the ultimate moment M_n can be computed. The study by Desayi and Krishnan (1964) revealed that the stress-strain relation is divided into two parts as follows:

1) When concrete strain is $\varepsilon_c < 0.002$

$$\frac{f_c}{f_c'} = \frac{2\varepsilon_c}{0.002} - \left(\frac{\varepsilon_c}{0.002}\right)^2 \tag{9}$$

2) When concrete strain is $0.002<\varepsilon_c<0.003$

$$f_c / f_c' = 1 - 300(\varepsilon_c - 0.002) \tag{10}$$

where f_c=compression stress of concrete; $\varepsilon_c = f_c/E_c$.

This relationship is graphed in Fig.3. This stress-stain relation was proved to cover well most of the test results. Many of the test results in the second portion are very similar to a linear form. The suggestion of a linear form for the second portion is a simple and reliable model for concrete related research. The above relation is cited popularly in concrete research.

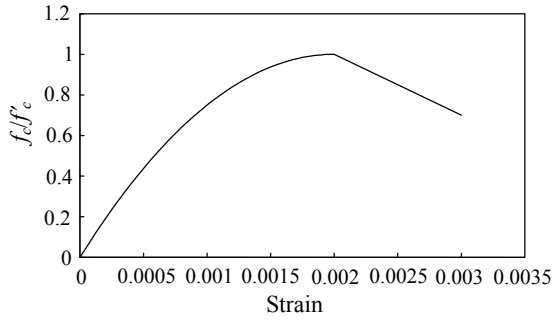

Fig.3 Concrete stress-strain relationship (Desayi and Krishnan, 1964)

According to Assumption (3), the failure is controlled by the GFRP sheet. If the ultimate fiber sheet strain is $(\varepsilon_{pl})_u$, referring to Fig.4 the concrete strain ε_c at any location z from N. A. is

$$\varepsilon_c = \frac{z}{(h+t_{pl}/2-x)}(\varepsilon_{pl})_u \tag{11}$$

where z is any arbitrary location of concrete; h, entire height of R. C. beam; t_{pl}, thickness of FRP plate.

1. If N. A. is in the flange area

N. A. located in the flange area means $x \le h_f$, as shown in Fig.4. Substituting Eq.(11) into Eqs.(9) or (10), the resultant force of concrete C_c is the summation of C_{c1} and C_{c2} where

$$C_{c1} = b\int_0^{x_1} f_c'\left(\frac{2(\varepsilon_{pl})_u z}{0.002\left(h+t_{pl}/2-x\right)} - \left(\frac{(\varepsilon_{pl})_u z}{0.002\left(h+t_{pl}/2-x\right)}\right)^2\right)\mathrm{d}z$$
$$0 \le z \le x_1 \tag{12}$$

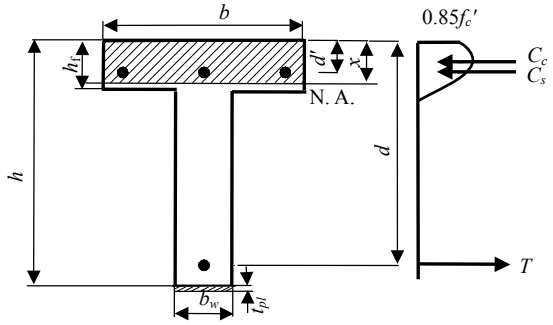

Fig.4 Stress distribution of T-shaped beams with GFRP sheets and with N. A. above h_f (in flange area)

$$C_{c2} = b\int_{x_1}^{x} f_c'\left(1 - 300\left(\frac{(\varepsilon_{pl})_u z}{h+t_{pl}/2-x} - 0.002\right)\right)\mathrm{d}z,$$
$$x_1 \le z \le x \tag{13}$$

where x_1 is the location where the concrete strain is 0.002; C_{c1}, compression force resultant of concrete when the neutral axis is located in the flange area and z is in the range of $0 \le z \le x_1$; C_{c2}, compression force resultant of concrete when the neutral axis is located in flange area and z is in range of $x_1 \le z \le x$.

The compressive steel stress is

$$\varepsilon_s' = \frac{\varepsilon_c^u (x - d')}{x} \tag{14}$$

According to the equilibrium equation $T=C$,

$$C_{c1} + C_{c2} + A_s' f_s' = A_s f_y + b_w t_{pl} E_{pl} (\varepsilon_{pl})_u$$

the neutral axis x can be determined, where E_{pl} is young's modulus of FRP plate. By substituting the x value into Eqs.(12), (13) and (14), the results for C_{c1} and C_{c2} can be computed and whether the compressive steel is yielding or not can be verified. The load acting locations for C_{c1} and C_{c2}, called $\overline{y}_1$ and $\overline{y}_2$, can be determined as follows

$$\overline{y}_1 = \left(b\int_0^{x_1} f_c'\left(\frac{2(\varepsilon_{pl})_u z}{0.002(h+t_{pl}/2-x)} - \left(\frac{(\varepsilon_{pl})_u z}{0.002(h+t_{pl}/2-x)}\right)^2\right)z\mathrm{d}z\right) \Big/ C_{c1} \tag{15}$$

$$\overline{y}_2=b\int_{x_1}^{x} f_c'\left(1-300\left(\frac{(\varepsilon_{pl})_u z}{h+t_{pl}/2-x}-0.002\right)\right)z\mathrm{d}z \Big/ C_{c2} \tag{16}$$

where $\overline{y}_1$ is acting location of force C_{c1}; $\overline{y}_2$ is acting location of force C_{c2}.

If the compressive steel is not yielding, the nominal moment M_n will be

$$M_n=A_s'f_s'(x-d')+A_sf_y(d-x)+C_{c1}\overline{y}_1 +C_{c2}\overline{y}_2+t_{pl}b_wE_{pl}(\varepsilon_{pl})_u(h+t_{pl}/2-x) \tag{17}$$

If the compressive steel is yielding, the nominal moment M_n will be

$$M_n=A_s'f_y(x-d')+A_sf_y(d-x)+C_{c1}\overline{y}_1+C_{c2}\overline{y}_2 +t_{pl}b_wE_{pl}\varepsilon_{pl}(h+t_{pl}/2-x) \tag{18}$$

2. If N. A. is in the web area

N. A. located in web area means $x\geq h_f$, as shown in Fig.5. In this case the concrete resultant force will be $C_c=(C_{c1})'+(C_{c2})'+(C_{c3})'+(C_{c4})'$, where

$$(C_{c1})'=b_w\int_0^{x_1} f_c'\left(\frac{2(\varepsilon_{pl})_u z}{0.002(h+t_{pl}/2-x)} -\left(\frac{(\varepsilon_{pl})_u z}{0.002(h+t_{pl}/2-x)}\right)^2\right)\mathrm{d}z \tag{19}$$

$$(C_{c2})'=b_w\int_{x_1}^{x} f_c'\left(1-300\left(\frac{(\varepsilon_{pl})_u z}{h+t_{pl}/2-x}-0.002\right)\right)\mathrm{d}z \tag{20}$$

$$(C_{c3})'=(b-b_w)\int_{h_f}^{x_1} f_c'\left(\frac{2(\varepsilon_{pl})_u z}{0.002(h+t_{pl}/2-x)} -\left(\frac{(\varepsilon_{pl})_u z}{0.002(h+t_{pl}/2-x)}\right)^2\right)\mathrm{d}z \tag{21}$$

$$(C_{c4})'=(b-b_w)\int_{x_1}^{x} f_c'\left(1-300\left(\frac{(\varepsilon_{pl})_u z}{h+t_{pl}/2-x}-0.002\right)\right)\mathrm{d}z \tag{22}$$

where $(C_{c1})'$ is compression force resultant of concrete in the part of b_w when the neutral axis is located in the web area and z is in the range of $0\leq z\leq x_1$; $(C_{c2})'$, compression force resultant of concrete in the part of b_w when the neutral axis is located in web area and z is in range of $x_1\leq z\leq x$; $(C_{c3})'$, compression force resultant of concrete in the part of $(b-b_w)$ when neutral axis is located in web area and z is in range of $0\leq z\leq x_1$; $(C_{c4})'$, compression force resultant of concrete in the part of $(b-b_w)$ when neutral axis is located in web area and z is in range of $x_1\leq z\leq x$.

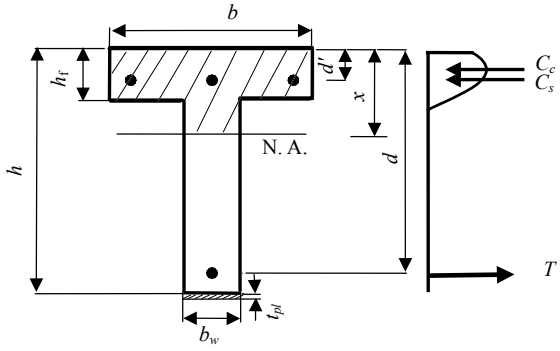

Fig.5 Stress distribution of T-shaped beams with GFRP sheets and with N. A. above h_f (in web area)

According to the equilibrium equation $T=C$,

$$(C_{c1})'+(C_{c2})'+(C_{c3})'+(C_{c4})'+A_s'f_s'=A_sf_y+E_{pl}t_{pl}b_w(\varepsilon_{pl})_u$$

N. A. location x can be determined. Substituting the x value into Eqs.(19)~(22), each concrete resultant force can be determined. Whether the compressive steel is yielding or not can also be verified with the x value. The resultant force acting locations, called $\overline{y}_1'$, $\overline{y}_2'$, $\overline{y}_3'$ and $\overline{y}_4'$ can be derived as

$$\overline{y}_1'=\left(b_w\int_0^{x_1} f_c'\left(\frac{2(\varepsilon_{pl})z}{0.002(h+t_{pl}/2-x)} -\left(\frac{(\varepsilon_{pl})z}{0.002(h+t_{pl}/2-x)}\right)^2\right)z\mathrm{d}z\right)\Big/(C_{c1})' \tag{23}$$

$$\overline{y}_2'=\left(b_w\int_{x_1}^{x} f_c'\left(1-300\left(\frac{(\varepsilon_{pl})\ z}{h+t_{pl}/2-x}-0.002\right)\right)z\mathrm{d}z\right)\Big/(C_{c2})' \tag{24}$$

$$\bar{y}_3'=\left((b-b_w)\int_{h_f}^{x_1} f_c'\left(\frac{2(\varepsilon_{pl})z}{0.002(h+t_{pl}/2-x)}-\left(\frac{(\varepsilon_{pl})z}{0.002(h+t_{pl}/2-x)}\right)^2\right)\mathrm{d}z\right)\Big/(C_{c3})' \tag{25}$$

$$\bar{y}_4'=\left((b-b_w)\times\int_{x_1}^{x} f_c'\left(1-300\left(\frac{(\varepsilon_{pl})z}{h+t_{pl}/2-x}-0.002\right)\right)z\mathrm{d}z\right)\Big/(C_{c4})' \tag{26}$$

where $\bar{y}_1'$ is acting location of force $(C_{c1})'$; $\bar{y}_2'$, acting location of force $(C_{c2})'$; $\bar{y}_3'$, acting location of force $(C_{c3})'$; $\bar{y}_4'$, acting location of force $(C_{c4})'$.

If the compressive steel is not yielding, the ultimate moment M_n will be

$$M_n=A_s'f_s'(x-d')+A_sf_y(d-x)+t_{pl}b_wE_{pl}(\varepsilon_{pl})_u(h+t_{pl}/2-x)+(C_{c1})'\bar{y}_1'+(C_{c2})'\bar{y}_2'+(C_{c3})'\bar{y}_3'+(C_{c4})'\bar{y}_4' \tag{27}$$

If the compressive steel is yielding, the ultimate moment M_n will be

$$M_n=A_s'f_y(x-d')+A_sf_y(d-x)+t_{pl}b_wE_{pl}(\varepsilon_{pl})_u(h+t_{pl}/2-x)+(C_{c1})'\bar{y}_1'+(C_{c2})'\bar{y}_2'+(C_{c3})'\bar{y}_3'+(C_{c4})'\bar{y}_4' \tag{28}$$

Analytical method for T-shaped beams with PGFRP sheets

Using PGFRP sheets to rehabilitate R. C. or P. C. beams can strengthen the beams and also camber them. Therefore, under the same load conditions, beams with PGFRP sheets have smaller deflections than those with normal GFRP sheets. If the assumptions are that the beams always fail on the tension faces, the nominal moment capacities for beams with PGFRP sheets will be the same as those for beams with GFRP sheets.

Analytical method for ⊥-shaped beams without GFRP sheets

For ⊥-shaped beams without GFRP sheets, the compression distribution on the concrete is assumed to be a rectangular shape, as shown in Fig.6.

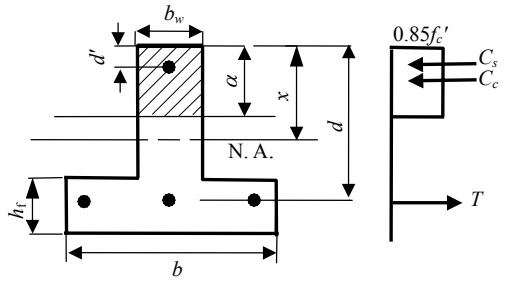

Fig.6 Compression distribution of ⊥-shaped beams without GFRP sheets

If the strain of the compressed steel is $\varepsilon_s'=\dfrac{\varepsilon_c^u(x-d')}{x}<\varepsilon_y$, the steel stress will be $f_s'=E_s\varepsilon_s'$.

According to equilibrium equation $C_c+C_s=T$,

$$0.85f_c'b_w\beta_1x+A_s'E_s\frac{\varepsilon_c^u(x-d)}{x}=A_sf_y \tag{29}$$

the value of x can be determined. The nominal moment is then,

$$M_n=0.85f_c'b_w\beta_1x(d-\beta_1x/2)+A_s'f_s'(d-d') \tag{30}$$

If the strain of the compressed steel is yielding, meaning ε_s' is greater than ε_y, the steel stress will be $f_s'=f_y$.

According to equilibrium equation $C_c+C_s=T$,

$$0.85f_c'b_w\beta_1x+A_s'f_y=A_sf_y \tag{31}$$

the value of x can be determined. The nominal moment is then,

$$M_n=0.85f_c'b_w\beta_1x(d-\beta_1x/2)+A_s'f_y(d-d') \tag{32}$$

Analytical method for ⊥-shaped beams with GFRP sheets

For ⊥-shaped beams with GFRP sheets, the compression distribution on the concrete is also assumed to have a rectangular shape, as shown in Fig.7.

The following assumptions are made for determining the nominal moment for ⊥-shaped beams with

GFRP sheets: (1) The GFRP sheet and concrete interface is well bonded and the GFRP sheets will never fail; (2) The strengthened beams fail on the compression faces (top faces); (3) The ultimate concrete strain is ε_c^u=0.003; (4) All of the tension steel yields.

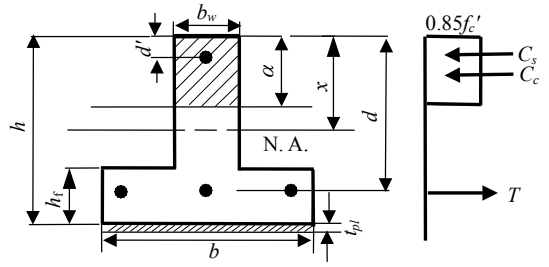

Fig.7 Compression distribution of ⊥-shaped beams with GFRP sheets

Based on these assumptions, the GFRP sheet strain ε_{pl} should be

$$\varepsilon_{pl}=\frac{(h-x+t_{pl}/2)\varepsilon_c^u}{x} \tag{33}$$

and the compressive steel strain should be

$$\varepsilon_s'=(x-d')\varepsilon_c^u/x \tag{34}$$

Based on the equilibrium equation T=C,

$$0.85f_c'b_w\beta_1x+\varepsilon_s'E_sA_s'=A_sf_y+\varepsilon_{pl}E_{pl}bt_{pl} \tag{35}$$

and substituting Eqs.(33) and (34) into Eq.(35),

$$\begin{aligned}&0.85f_c'b_w\beta_1x^2+\left(A_s'E_s\varepsilon_c^u-A_sf_y+E_{pl}bt_{pl}\varepsilon_c^u\right)x\\&-\left(A_s'E_s\varepsilon_c^ud'+\left(h+t_{pl}/2\right)E_{pl}bt_{pl}\varepsilon_c^u\right)=0\end{aligned} \tag{36}$$

the value of x can be determined from Eq.(36). The x value is substituted into Eq.(34) to check whether the compressive steel is yielding or not and into Eq.(33) to determine the GFRP sheet stress.

If the compression steel is not yielding, the nominal moment will be

$$\begin{aligned}M_n=&A_sf_y\left(d-x\right)+E_{pl}\varepsilon_{pl}bt_{pl}\left(h+t_{pl}/2-x\right)\\&+A_s'f_s'\left(x-d'\right)+0.85f_c'b_w\beta_1x\left(x-\beta_1x/2\right)\end{aligned} \tag{37}$$

If the compression steel is yielding, the nominal moment will be the same as Eq.(37) but f_s' must be changed into $f_{y.}$

Analytical method for ⊥-shaped beams with PGFRP sheets

Based on the assumption that the strengthened beams (⊥-shaped beams) fail on the compression faces (top faces), the nominal moments M_n for ⊥-shaped beams can be computed by directly adding Pe to Eq.(37) in which P is the preload and e is the eccentric distance of the preload P from the beam centroid.

COMPARISON OF ANALYSIS AND TEST RESULTS

The test setup in Part I of this paper is schematically shown in Fig.7 in (Huang *et al*., 2005). The analytical (based on the data in Table 1) and experimental results are compared using the ultimate concentrated loads. All the analytical results for the test specimens are computed using the analytical method developed in this article. The comparisons of analytical and experimental results are listed in Table 2.

Table 1 Properties of GFRP sheets, steel and concrete

Property	GFRP sheet	Steel	Concrete
Sheet thickness/ply (mm)	1.30		
Strength (MPa)	460	460	28
Young's modulus (GPa)	23	204	20.4

The strength for GFRP sheet and steel is tensile strength and for concrete is compressive strength

Table 2 Analytical and experimental ultimate loads

Beams	P_E (kN)	P_A (kN)	Percentage of difference $[P_E-P_A]/P_A$
TRB	16.0	18.3	−12.6%
TFB	24.8	47.2	−47.5%
TPFB	32.0	47.2	−32.2%
TPUFB	52.0	47.2	+10.2%
⊥RB	31.5	50.3	−37.4%
⊥FB	62.2	78.2	−20.5%
⊥PFB	68.5	80.0	−14.4%

P_E: Experimental results; P_A: Analytical results

Comparisons for T-shaped beams

The nomenclature for the tested T-shaped beams is shown in Fig.2 in (Huang *et al*., 2005). According to Table 2, the percentage of difference between experimental and analytical results ranges from 10% to 48%. Beam TFB had 47.5% difference and Beam TPFB had 32.2% difference. The reason that these two beams had large difference may be that the T-shaped beams have very narrow bottom face for GFRP sheet to be bonded and that the GFRP sheets were simply bonded onto the narrow bottom faces. This simple bonding way gave the beam much less ultimate load than that computed by the analytical method. However, in beam TPUFB, referring to Fig.8, the GFRP sheet is not only bonded onto the beam's bottom face but also rolled around the corner and bonded onto the web's two vertical sides (called U-shape bonding). The U-shape bonding beam, Beam TPUFB, can even exceed its analytical value by 10.2 %. In the process of making U-shape bonding, both corners of the beam should be smoothed before the GFRP sheets are bonded onto the beam to avoid fracturing the GFRP sheets. It is suggested that for a beam with a narrow face for GFRP sheets to bond should be bonded in U-shape bonding way instead of simply bonded onto the narrow face.

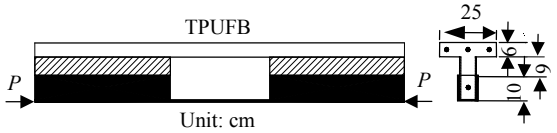

Fig.8 U-shaped bonding in Beam TPUFB

Comparisons for ⊥-shaped beams

The nomenclature for the tested ⊥-shaped beams is shown in Fig.4 in (Huang *et al*., 2005). For these ⊥-shaped beams, Beam ⊥FB was bonded by GFRP sheets in U-shape bonding way but Beam ⊥PFB was bonded by GFRP sheets simply on its bottom face. According to Table 2, these two beams' differences between experimental and analytical results are within 21%. These differences are far less than those in Beam TFB and Beam TPFB. This comparison shows that for a beam with a wide face for GFRP sheets to be bonded, its experimental ultimate load will be closer to its analytical ultimate load no matter whether the U-shape bonding way is used or not. Finally, Beam ⊥RB has large difference, for which there is no good explanation yet. According to Table 2, all the differences for beams except Beams TFB, TPFB, and ⊥RB are within 21%. For the sake of safety, this paper suggests to decrease the differences to 20% of the analytical strength for the engineering purposes.

CONCLUSIONS AND SUGGESTIONS

According to the analytical results and comparisons with the corresponding experimental results, the proposed analytical method for T (under-strengthened beams) and ⊥-shaped beams (over-strengthened beams) with/without GFRP sheets is suggested for computing the load-carrying capacities (ultimate loads). The following conclusions and suggestions are also made:

1. For a beam with a narrow face for bonding to GFRP sheets, a U-shape bonding is suggested so that the loading capacity of the strengthened beam will be close to the present analytical results.

2. For a beam with a wide face for bonding to GFRP sheets, the loading capacities of the strengthened beams will be closer to the present analytical results no matter whether the U-shape bonding is used or not.

3. For the sake of safety, a 20% decrease of the analytical loading capacities is suggested for engineering purposes.

References

ACI Committee 440, 1996. State-of-the-art Report on Fiber Reinforced Plastic (FRP) Reinforcement for Concrete Structures (ACI 440R-96). American Concrete Institute, Farmington Hills, Michigan, p.65.

ACI Committee 318, 1999. Building Code Requirements for Structural Concrete (ACI 318-99) and Commentary (318R-99). American Concrete Institute, Farmington Hills, Michigan, p.391.

An, W., Saadatmanesh, H., Ehan, M.R., 1991. RC beams strengthened with GFRP plates: Part II: analysis and parametric study. *Journal of Structural Engineering*, *ASCE*, **117**(11):3434-3455.

CHBDC, 2000. Canadian Highway Bridge Design Code. CAN/CSA-S6-00, CSA International, Toronto, Ontario, Canada.

Desayi, P., Krishnan, S., 1964. Equation for the stress-strain curve of concrete. *Journal of the American Concrete Institute ACI*, **61**(3):345-350.

Garden, H.N., Hollaway, L.C., Thorne, A.M., Parke, G.A.R.,

1996. A Parameter Study of the Strengthening of Reinforced Concrete Beams with Bonded Composites. Proceedings of the Third International Conference on Bridge Management, Guildford, p.400-408.

Grace, B.F., Singh, S.B., 2003. Design approach for carbon fiber-reinforced polymer prestressed concrete beams. *ACI Structural Journal*, **100**(3):365-376.

Huang, Y.L., Wu, J.H., Yen, T., Hung, C.H., Lin, Y.C., 2005. Strengthening reinforced concrete beams using prestressed glass fiber-reinforced polymer–Part I: Experimental study. *Journal of Zhejiang University SCIENCE*, **6A**(3):166-174.

JSCE (Japan Society of Civil Engineers), 1997. Recommendation for Design and Construction of Concrete Structures Using Continuous Fiber Reinforcing Materials. Concrete Engineering Series 23, Research Committee on Continuous Fiber Reinforcing Materials, Tokyo, Japan, p.325.

Raithby, K.D., 1980. External Strengthening of Concrete Bridges with Bonded Steel Plates. Transport and Road Research Laboratory, Supplemental Report, p.612.

Saadatmanesh, H., Ehsani, M., 1991. R. C. beams strengthened with GFRP plates–part I: experimental study. *Journal of Structural Engineering*, *ASCE*, **117**(11):3417-3433.

Triantafillou, T.C., Deskovic, N., Deuring, M., 1992. Strengthening of concrete structures with prestressed fiber reinforced plastic sheets. *ACI Structural Journal*, **89**(3):235-244.

Wang, C.K., Salmon, C.G., 1998. Reinforced Concrete Design, Sixth Edition. Addition Wesley Longman.

Wong, R.S.Y., Vecchio, F.J., 2003. Towards modelling of reinforced concrete members with externally bonded fiber-reinforced polymer composites. *ACI Structural Journal*, **100**(1):47-55.